

An asymptotically compatible unfitted finite element methods for nonlocal elliptic Interfaces: local limits and sharp error estimates

Haixia Dong^a, Ziqing Xie^a, Jiwei Zhang^{b,*}

^aMOE-LCSM, School of Mathematics and Statistics, Hunan Normal University, Changsha, Hunan 410081, P. R. China.

^bCorresponding author. School of Mathematics and Statistics, and Hubei Key Laboratory of Computational Science, Wuhan University, Wuhan 430072, China

Abstract

This paper presents the development and analysis of an asymptotically compatible (AC) unfitted finite element method for one-dimensional nonlocal elliptic interface problems. The proposed method achieves optimal error estimates through three principal contributions: (i) an extended maximum principle, coupled with an asymptotic consistency analysis of the flux operator, which establishes second-order convergence of nonlocal solutions to their local counterparts in the maximum norm; (ii) a Nitsche-type formulation that directly incorporates nonlocal jump conditions into the weak form, enabling high accuracy without body-fitted meshes; and (iii) a rigorous proof of optimal convergence rates in both the energy and L^2 norms via the nonlocal maximum principle, flux consistency, and a newly derived nonlocal Poincaré inequality. Numerical experiments confirm the theoretical findings and demonstrate the robustness and efficiency of the proposed approach, thereby providing a foundation for extensions to higher dimensions.

Keywords: nonlocal elliptic interface problems, unfitted finite element methods, asymptotically compatible schemes, error estimates, jump conditions

1. Introduction

Nonlocal models (NLMs) have become indispensable tools for simulating long-range interactions and multiscale material behavior, with applications spanning fracture mechanics [1, 2], damage evolution [3, 4], and crack propagation [5, 6, 7]. Unlike classical local models, NLMs employ integral formulations that naturally capture nonlocal effects and relax the stringent regularity requirements on field variables, making them particularly suitable for problems involving discontinuities and singularities.

Building on these advantages, this work focuses on one-dimensional nonlocal elliptic interface (NLI) problems, where solutions exhibit discontinuities across interfaces. Specifically, we consider the domain $\Omega = (a, b)$ with an interface point $\Gamma_0 = \alpha$ that divides Ω into two subdomains $\Omega_1 = (a, \alpha)$ and $\Omega_2 = (\alpha, b)$.

*Corresponding author

Email address: jiweizhang@whu.edu.cn (Jiwei Zhang)

To characterize nonlocal interactions, we introduce two horizon parameters δ_1 and δ_2 with $\delta_1 \leq \delta_2$, and define the interaction intervals as follows

- $\mathcal{I}_1^D = (a - \delta_1, a)$ and $\mathcal{I}_2^D = (b, b + \delta_2)$ for Dirichlet-type nonlocal interactions;
- $\mathcal{I}_1^J = (\alpha, \alpha + \delta_1)$ and $\mathcal{I}_2^J = (\alpha - \delta_2, \alpha)$ for interface interactions.

The nonlocal interface Γ is defined as the union of the interaction zones: $\Gamma = \mathcal{I}_1^J \cup \mathcal{I}_2^J = (\alpha - \delta_2, \alpha + \delta_1)$. The complete interaction domains are denoted by $\mathcal{I}_1 = \mathcal{I}_1^D \cup \mathcal{I}_1^J$ for Ω_1 and $\mathcal{I}_2 = \mathcal{I}_2^D \cup \mathcal{I}_2^J$ for Ω_2 , with the nonlocal Dirichlet boundary given by $\mathcal{I}^D = \mathcal{I}_1^D \cup \mathcal{I}_2^D$. For scalar functions $u_i : \Omega_i \cup \mathcal{I}_i \rightarrow \mathbb{R}$ ($i = 1, 2$), the nonlocal operators are defined as

$$\mathcal{L}_i u_i(x) = \int_{\Omega_i \cup \mathcal{I}_i} [u_i(x) - u_i(y)] \gamma_{\delta_i}(x, y) dy, \quad x \in \Omega_i,$$

where the kernel function $\gamma_{\delta_i}(x, y)$ satisfies

$$\gamma_{\delta_i}(x, y) : \mathbb{R} \times \mathbb{R} \rightarrow \mathbb{R}^+, \quad \gamma_{\delta_i}(x, y) = \gamma_{\delta_i}(y, x), \quad \gamma_{\delta_i}(x, y) = 0, \quad |x - y| > \delta_i > 0. \quad (1)$$

We consider a rescaled kernel $\bar{\gamma}_{\delta_i}(s) = \delta_i^{-3} \gamma_i(s/\delta_i)$, where γ_i is a nonnegative, radially symmetric function that is locally integrable and compactly supported within $|s| < 1$, and satisfies the moment condition

$$\frac{1}{2} \int_{-1}^1 s^2 \gamma_i(s) ds = \sigma_i > 0, \quad i = 1, 2. \quad (2)$$

The nonlocal interface (NLI) problem is to find solutions u_i ($i = 1, 2$) satisfying

$$\mathcal{L}_i u_i = f_i, \quad x \in \Omega_i, \quad \text{and} \quad u_i = g_i, \quad x \in \mathcal{I}_i^D, \quad (3)$$

with interface conditions

$$u_2 - u_1 = \varphi, \quad x \in \Gamma, \quad \text{and} \quad \mathcal{F}(u_1, u_2) = \psi, \quad x \in \Gamma \cup \Omega_2^J. \quad (4)$$

Here, $\Omega_2^J = (\alpha + \delta_1, \alpha + \delta_2)$ represents an extended interaction zone, and the interface-flux operator $\mathcal{F}(u_1, u_2)$ is defined piecewise as in [8]

$$\mathcal{F}(u_1, u_2) = \begin{cases} \int_{\Omega_2^J} [u_2(x) - u_2(y)] \gamma_{\delta_2}(x, y) dy \\ \quad + \frac{1}{2} \int_{\mathcal{I}_1^J} [u_1(x) - u_1(y)] (\gamma_{\delta_2}(x, y) - \gamma_{\delta_1}(x, y)) dy, & x \in \mathcal{I}_2^J, \\ \frac{1}{2} \int_{\mathcal{I}_2^J} [u_2(x) - u_2(y)] (\gamma_{\delta_1}(x, y) - \gamma_{\delta_2}(x, y)) dy, & x \in \mathcal{I}_1^J. \end{cases} \quad (5)$$

A central challenge in NLI problems is twofold: ensuring the nonlocal solution converges to the classical local solution as nonlocal effects vanish (i.e., $\delta_1, \delta_2 \rightarrow 0$), and developing efficient numerical methods capable of handling interfacial discontinuities without compromising accuracy or computational efficiency.

This challenge raises a fundamental question in nonlocal modeling: whether nonlocal interface equations indeed converge to a classical local interface problem as the nonlocal effect vanishes. This limiting behavior, known as the *local limit*, is essential for practical applications of nonlocal models, especially in multiscale modeling and simulations, such as when macroscopic structures are influenced by microscopic nonlocal effects. Various analytical techniques have been employed to study this convergence, including Taylor expansions [1, 9], functional analysis [10, 11, 12], and maximum principles [13, 14]. Nevertheless, existing studies often lack proofs of local limit convergence in the maximum norm under realistic regularity assumptions, leaving a gap in solution stability analysis.

Another crucial aspect is the asymptotic compatibility (AC) of numerical discretizations, that is whether discrete approximations also converge to the corresponding local limit as both the nonlocal horizon and mesh size tend to zero. A significant advance was made by Tian and Du, who introduced the AC framework [15, 16]. This concept has since been generalized to Neumann-type constraints [17], spectral methods on periodic domains [18, 19], discontinuous Galerkin schemes [20, 21], nonlocal space–time models [22], and advanced gradient-recovery techniques [23]. Recent contributions [24, 25] improved convergence analysis for finite element approximations with approximated interaction neighborhoods. However, many of these extensions either depend on specialized mesh structures or do not explicitly incorporate nonlocal jump conditions, thereby restricting their utility for NLI problems.

Although classical interface problems have been widely studied using techniques such as the immersed boundary method [26, 27], extended/cut finite element method [28, 29] and immersed interface method [30, 31, 32], numerical approaches for NLI problems remain less developed. Early formulations for NLI problems were established in [35, 36], yet they lacked rigorous error analysis. Subsequent works [37] established well-posedness and convergence under conforming discretizations, which can be computationally expensive for complex interfaces. State-based peridynamic models [38, 39] have addressed certain discontinuity issues but generally fail to achieve AC. More recently, [8] explored local limits and asymptotically compatible formulations for nonlocal interface problems with jumps. Despite these efforts, several key questions remain open: However, several critical issues remain unresolved: (1) Can the local limit with respect to δ be rigorously proven in the maximum norm under practical regularity assumptions? (2) What is the optimal convergence rate with respect to δ for the continuum nonlocal models? (3) Is it possible to construct a theoretical framework that establishes the optimal convergence order for an AC unfitted finite element scheme applied to NLI problems?

Motivated by these open questions outlined above and the practical need to model engineering problems involving inherent discontinuities, such as fracture in composite materials or dynamic damage evolution, this work develops a robust AC unfitted finite element method (FEM) on a Cartesian grid for one-dimensional nonlocal elliptic interface problems. In contrast to previous approaches [37, 8], which often rely on conforming discretizations, the proposed method directly embeds the nonlocal jump condi-

tions into the weak formulation via a Nitsche-type approach. This allows the use of a single Cartesian background mesh, greatly simplifying implementation and improving computational efficiency. The main contributions of this work are summarized as follows:

(1) Local limit analysis in the maximum norm. An extended maximum principle is established for NLI problems, providing explicit control over solution behavior through the flux operator $\mathcal{F}(u_1, u_2)$. Combined with a rigorous asymptotic consistency analysis showing $\mathcal{F}(u_1, u_2) = \sigma_1 u_1'(\alpha) - \sigma_2 u_2'(\alpha) + \mathcal{O}(\max(\delta_1^2, \delta_2^2))$, this work proves second-order convergence of nonlocal solutions to the local limit, i.e., $\|u - u_0\|_{\infty, \Omega_1 \cup \Omega_2} \leq C \max(\delta_1^2, \delta_2^2)$. This result fills a notable gap in the maximum-norm convergence analysis for nonlocal interface models.

(2) Asymptotically compatible unfitted FEM scheme. A Nitsche-type variational formulation is proposed to directly embed nonlocal jump conditions into the weak form, thereby avoiding the need for body-fitted meshes. Computational efficiency is further improved via a novel block matrix decomposition strategy and an exact integration technique using linear transformations to reference elements. The resulting method preserves asymptotic compatibility while achieving optimal convergence rates, even for problems with discontinuous solutions across interfaces.

(3) Optimal $(k + 1)$ -order convergence analysis. The convergence of the proposed scheme is rigorously established, achieving order $(k + 1)$ in both the energy and L^2 -norms

$$\|u - u^h\|_{\delta} \leq C \max\{\delta_1^{-1}, \delta_2^{-1}\} h^{k+1}, \quad \|u - u^h\|_{L^2} \leq C \max\{\delta_1^{-1}, \delta_2^{-1}\} h^{k+1}.$$

The analysis accommodates arbitrary polynomial degree k , allows non-matching horizon parameters $\delta_1 \neq \delta_2$, and accurately captures solution jumps at multiple interfaces. Numerical experiments validate the robustness and high accuracy of the proposed scheme.

The paper is organized as follows. Section 2 develops the maximum principle for nonlocal interface problems and proves second-order convergence to local limit under suitable constrained volume conditions. Section 3 presents the asymptotically compatible unfitted finite-element method and derives corresponding optimal error estimates. Section 4 provides numerical validation. Conclusions are given in Section 5, and detailed proofs are collected in the Appendix.

2. The convergence limits from the nonlocal solutions to local solutions

2.1. Maximum principle for nonlocal interface problem

Maximum principle plays a central role in our analysis. Although well-established for local elliptic interface problems, its nonlocal counterpart must account for long-range interactions and interface jump conditions. We therefore establish a maximum principle for nonlocal elliptic interface problems to control the pointwise behavior of solutions.

To quantify the solution regularity, we introduce the space of bounded continuous functions $C_b(\Omega) := \{u \in C(\Omega) : u \text{ is bounded}\}$, equipped with the supremum norm $\|u\|_{\infty, \Omega} := \sup_{x \in \Omega} |u(x)|$. Its natural extension to higher regularity is defined as $C_b^m(\Omega) := \{u^{(k)} \in C_b(\Omega) : \forall \text{ nonnegative integer } k \leq m\}$ for any integer $m \geq 0$, endowed with the norm $\|u_i\|_{C_b^m(\Omega_i)} := \max_{0 \leq k \leq m} \|u_i^{(k)}\|_{\infty, \Omega_i}$. For the interface problem, we further introduce the trace norm $\|u\|_{\infty, b} := \sup_{x \in b} |u(x)|$, where $b = \Gamma, \mathcal{I}_1^D$ or \mathcal{I}_2^D , to capture the behavior of the solution on the interface and Dirichlet boundaries. The global solution is measured by $\|u\|_{\infty, \Omega} = \max_{i=1,2} \|u_i\|_{\infty, \Omega_i}$, providing a uniform control across subdomains. Endowed with these norms, the product space $C_b(\Omega_1) \times C_b(\Omega_2)$ forms a Banach space, which serves as the functional framework for establishing the nonlocal maximum principle and related interface properties.

Theorem 2.1. Let $\Omega = (a, b)$ be partitioned into $\Omega_1 = (a, \alpha)$ and $\Omega_2 = (\alpha, b)$, and let $\delta_1, \delta_2 > 0$ be horizon parameters. Suppose $u_i \in C(\Omega_i \cup \mathcal{I}_i)$ for $i = 1, 2$ satisfying (i) $\mathcal{L}_i u_i \leq 0$ in Ω_i ; (ii) $u_1(x) = u_2(x)$, $\forall x \in \Gamma$; and (iii) $\mathcal{F}(u_1, u_2)(x) \leq 0, \forall x \in \Gamma$. Then the global maximum of u is bounded by

$$\|u\|_{\infty, \Omega_1 \cup \Omega_2} \leq \max \left(\|u_1\|_{\infty, \mathcal{I}_1^D}, \|u_2\|_{\infty, \mathcal{I}_2^D} \right).$$

Proof. Suppose u attains a positive maximum M at some point $x_0 \in \Omega_1$ and assume this maximum is not achieved on \mathcal{I}_1^D . Since $u_1(x_0) = M \geq u_1(y)$ for all $y \in \Omega_1 \cup \mathcal{I}_1$, the nonlocal operator $\mathcal{L}_1 u_1(x)$ evaluated at x_0 satisfies

$$\mathcal{L}_1 u_1(x_0) = \int_{\Omega_1 \cup \mathcal{I}_1} [u_1(x_0) - u_1(y)] \gamma_{\delta_1}(x_0, y) dy \geq 0.$$

On the other hand, condition (i) implies $\mathcal{L}_1 u_1(x_0) \leq 0$, so it follows that $\mathcal{L}_1 u_1(x_0) = 0$. This equality forces $u_1(y) = M$ for all $y \in B_{\delta_1}(x_0) \cap (\Omega_1 \cup \mathcal{I}_1)$. By continuity, $u_1 \equiv M$ in a neighborhood of x_0 . From condition (ii), it follows that $u_2(\alpha) = u_1(\alpha) = M$.

Now consider $x \in \mathcal{I}_1^J$. A direct calculation shows that the flux operator satisfies

$$\mathcal{F}(u_1, u_2)(x) = \frac{1}{2} \int_{\mathcal{I}_2^J} [u_2(x) - u_2(y)] (\gamma_{\delta_2} - \gamma_{\delta_1}) dy = \frac{1}{2} \int_{\mathcal{I}_2^J} [u_2(x) - M] (\gamma_{\delta_2} - \gamma_{\delta_1}) dy \leq 0.$$

The sign-indefinite nature of $\gamma_{\delta_2} - \gamma_{\delta_1}$ forces $u_2(x) = M$ throughout \mathcal{I}_1^J . Similarly, for any $x \in \mathcal{I}_2^J$, the flux condition $\mathcal{F}(u_1, u_2)(x) \leq 0$ implies $\int_{\Omega_2^J} [u_2(x) - u_2(y)] \gamma_{\delta_2}(x, y) dy \leq 0$. Since $u_2(x) = M \geq u_2(y)$, equality holds if and only if $u_2(y) = M$ for all $y \in \Omega_2^J$.

For $x \in \Omega_2$ with $\text{dist}(x, \alpha) \leq \delta_2$, the nonlocal operator $\mathcal{L}_2 u_2(x)$ becomes

$$\mathcal{L}_2 u_2(x) = \int_{\Omega_2 \cup \mathcal{I}_2} [u_2(x) - u_2(y)] \gamma_{\delta_2}(x, y) dy = \int_{\Omega_2 \cup \mathcal{I}_2} [M - u_2(y)] \gamma_{\delta_2}(x, y) dy \leq 0.$$

Any value $u_2(y) > M$ would lead to $\mathcal{L}_2 u_2(x) > 0$, contradicting the inequality. Hence $u_2(y) = M$ for all $y \in \Omega_2 \cup \mathcal{I}_2$. Finally, if $u_2(x) < M$ for some $x \in \mathcal{I}_2^D$, then

$$\mathcal{L}_2 u_2(x) = \int_{b-\delta_2}^{b+\delta_2} [u_2(x) - u_2(y)] \gamma_{\delta_2}(x, y) dy = \int_{b-\delta_2}^{b+\delta_2} [u_2(x) - M] \gamma_{\delta_2}(x, y) dy < 0,$$

which contradicts the condition (i). Therefore, the maximum M must occur on \mathcal{I}_2^D . \square

To clearly distinguish the present results from both nonlocal formulations and their local counterparts, pointwise a priori estimates are now presented.

Theorem 2.2. Under the same assumptions as Theorem 2.1, with additional regularity condition that $u_i \in C_b^2(\Omega_i \cup \mathcal{I}_i^D)$ for $i = 1, 2$, there exists a constant $C = C(\gamma_1, \gamma_2, |\Omega|)$, independent of the horizon parameters δ_1 and δ_2 such that the following estimate holds

$$\|u\|_{\infty, \Omega} \leq C(\|u\|_{\infty, \mathcal{I}^D} + \|\mathcal{L}u\|_{\infty, \Omega} + \|\mathcal{F}(u_1, u_2)\|_{\infty, \Gamma}).$$

Proof. An auxiliary function $v(x)$ is constructed piecewise on $\Omega \cup \mathcal{I}^D$ as follows

$$v(x) = \begin{cases} v_1(x) = A_1 + B_1|x - \alpha|^2 + \epsilon\phi_1(x), & x \in \Omega_1 \cup \mathcal{I}_1^D, \\ v_2(x) = A_2 + B_2|x - \alpha|^2 + \epsilon\phi_2(x), & x \in \Omega_2 \cup \mathcal{I}_2^D, \end{cases}$$

where $A_i = \|u_i\|_{\infty, \mathcal{I}_i^D} + |\Omega|^2/2\sigma_i$ controls the boundary values, $B_i = -1/2\sigma_i < 0$, $\phi_i \in C_b^2(\Omega_i \cup \mathcal{I}_i^D)$ satisfies $\mathcal{L}_i\phi_i = 1$ with $\phi_i|_{\mathcal{I}_i^D} = 0$, and $\epsilon > 0$ is a parameter to be determined. By the nonlocal maximum principle [13] and the condition $\mathcal{L}_i\phi_i = 1$ with $\phi_i|_{\mathcal{I}_i^D} = 0$, there exists a constant $C_\phi = C_\phi(\gamma_i)$ such that $\|\phi_i\|_{\infty, \Omega_i} \leq C_\phi$.

Now define $w_i = u_i - v_i$. On the Dirichlet boundary \mathcal{I}_i^D ,

$$v_i(x)|_{\mathcal{I}_i^D} = A_i + B_i|x - \alpha|^2 \geq \left(\|u_i\|_{\infty, \mathcal{I}_i^D} + \frac{|\Omega|^2}{2\sigma_i}\right) - \frac{|\Omega|^2}{2\sigma_i} = \|u_i\|_{\infty, \mathcal{I}_i^D} \geq u_i(x)|_{\mathcal{I}_i^D},$$

which implies $w_i \leq 0$ on \mathcal{I}_i^D . Within Ω_i , noting that $\mathcal{L}_i A_i = 0$, $\mathcal{L}_i \phi_i = 1$, and

$$B_i \mathcal{L}_i(|x - \alpha|^2) = B_i \int_{\Omega_i \cup \mathcal{I}_i} [|x - \alpha|^2 - |y - \alpha|^2] \gamma_{\delta_i}(x, y) dy = -2B_i \sigma_i = 1,$$

it follows that

$$\mathcal{L}_i w_i = \mathcal{L}_i u_i - \left(\mathcal{L}_i(A_i + B_i|x - \alpha|^2) + \epsilon \mathcal{L}_i \phi_i\right) = \mathcal{L}_i u_i - (1 + \epsilon) \leq 0.$$

By the linearity of flux operator \mathcal{F} and integrability of γ_{δ_i} , the estimate $|\mathcal{F}(w_1, w_2)| \leq C_F \epsilon$ hold, where C_F depends on $\|\phi_i\|_{\infty}$ and γ_{δ_i} . Choosing $\epsilon = (\|\mathcal{F}(u_1, u_2)\|_{\infty, \Gamma} + \|\mathcal{L}_i u_i\|_{\infty, \Omega_i})/C_F$, yields

$$\mathcal{F}(w_1, w_2) \leq \mathcal{F}(u_1, u_2) + \mathcal{L}_i u_i \leq 0 \quad \text{on } \Gamma.$$

Applying the nonlocal interface maximum principle (Theorem 2.1), it is concluded that $w_i \leq 0$ in Ω_i , implying $u_i \leq v_i$. Therefore,

$$\|u_i\|_{\infty, \Omega_i} \leq \|v_i\|_{\infty, \Omega_i} = \max_{x \in \Omega_i} |A_i + B_i|x - \alpha|^2 + \epsilon\phi_i(x)| \leq A_i + \frac{|\Omega|^2}{2\sigma_i} + \epsilon C_\phi.$$

Substituting the expressions for ϵ and A_i gives

$$\|u_i\|_{\infty, \Omega_i} \leq \|u_i\|_{\infty, \mathcal{I}_i^D} + \frac{|\Omega|^2}{\sigma_i} + \frac{C_\phi}{C_F} (\|\mathcal{F}(u_1, u_2)\|_{\infty, \Gamma} + \|\mathcal{L}_i u_i\|_{\infty, \Omega_i}).$$

The constant C can be taken as $C = \max\left(1, \frac{|\Omega|^2}{\min(\sigma_1, \sigma_2)}, \frac{C_\phi}{C_F}\right)$, which depends on γ_i (through σ_i , C_ϕ , C_F) and $|\Omega|$, but remains independent of δ_1 and δ_2 . \square

2.2. Approximation order between nonlocal elliptic interface problem to its local counterpart

This subsection is devoted to analyzing the asymptotic convergence rate of the nonlocal solution u_i towards its local counterpart u_{0i} as the horizon parameter $\delta_i \rightarrow 0$. The corresponding local interface problem is given by

$$\mathcal{L}_i^0 u_{0i}(x) := -\sigma_i \frac{d^2 u_i(x)}{dx^2} = f_i(x), \quad x \in \Omega_i, \quad i = 1, 2, \quad (6)$$

subject to boundary conditions $u_{01}(a) = g_{01}$, $u_{02}(b) = g_{02}$, and interface conditions

$$[[u_0]] = 0, \quad \left[\left[\sigma \frac{\partial u_0}{\partial n} \right] \right] = \psi(x), \quad x \in \Gamma_0, \quad (7)$$

where $f_i \in C_b^2(\Omega_i)$ and σ takes the value σ_1 in Ω_1 and σ_2 in Ω_2 .

For a function $\hat{u}_i \in C_b^4(\Omega_i \cup \mathcal{I}_i)$, the nonlocal operator \mathcal{L}_i approximates the local operator \mathcal{L}_i^0 with second-order accuracy at any point $x \in \Omega_i$. As established in prior studies (e.g., [13, 40]), this relationship can be expressed as

$$\mathcal{L}_i \hat{u}_i(x) = \mathcal{L}_i^0 \hat{u}_i(x) + \mathcal{O}(\delta_i^2). \quad (8)$$

A natural question arises: does the interface flux operator $\mathcal{F}(u_1, u_2)$ exhibit analogous second-order convergence? An affirmative answer is essential to ensure consistency between the nonlocal and local interface formulations. The following lemma provides such a result.

Lemma 2.1. Let $\hat{u}_i \in C_b^4(\Omega_i \cup \mathcal{I}_i)$ for $i = 1, 2$. Assume the kernels $\{\gamma_{\delta_i}\}$ satisfies (1), (2) and

$$G(\gamma_{\delta_i}) := \sup_{x \in \Omega_i \cup \mathcal{I}_i} \int_{B_{\delta_i} \cap (\Omega_i \cup \mathcal{I}_i)} \gamma_{\delta_i}(x, y) dy \lesssim \delta_i^{-2}. \quad (9)$$

Then, for $x \in \Gamma$, the nonlocal flux operator $\mathcal{F}(u_1, u_2)$ converges to its local counterpart as

$$\mathcal{F}(\hat{u}_1, \hat{u}_2) = \sigma_1 \hat{u}'_1(\alpha) - \sigma_2 \hat{u}'_2(\alpha) + \mathcal{O}(\max(\delta_1^2, \delta_2^2)). \quad (10)$$

For clarity of exposition, the detailed proof is deferred to Appendix 6.1.

Theorem 2.3. Suppose $u_0 \in C_b^4(\Omega_1 \cup \Omega_2)$ is the unique solution to the local interface problem (6)-(7), and assume the family of kernels $\{\gamma_{\delta_i}\}$ satisfies (1), (2) and (9). Let u be the unique solution to the nonlocal interface problem (3)-(4) with boundary conditions constructed as

$$g_i(x) = g_{0i} + (x - x_i) \frac{du_{0i}}{dx}(x_i), \quad x_i = a \text{ or } b, \quad i = 1, 2.$$

Then there exists a constant $C > 0$, independent of δ_1, δ_2 , such that

$$\|u - u_0\|_{\infty, \Omega_1 \cup \Omega_2} \leq C \max(\delta_1^2, \delta_2^2).$$

Proof. Let \tilde{u}_0 be the piecewise fourth-order Taylor approximation of u_0 defined by

$$\tilde{u}_0(x) = \begin{cases} \sum_{m=0}^4 \frac{(x-a)^m}{m!} \partial_x^m u_{01}(a), & x \in \mathcal{I}_1^D, \\ u_{01}(x), & x \in \Omega_1, \\ u_{02}(x), & x \in \Omega_2, \\ \sum_{m=0}^4 \frac{(x-b)^m}{m!} \partial_x^m u_{02}(b), & x \in \mathcal{I}_2^D. \end{cases}$$

Since $u_0 \in C_b^4(\Omega_1 \cup \Omega_2)$, the extension \tilde{u}_0 belongs to $C_b^4(\mathcal{I}_1^D \cup \Omega_1 \cup \Omega_2 \cup \mathcal{I}_2^D)$.

For $x \in \Omega_i$, the second-order accuracy of the nonlocal operator (8) implies

$$\mathcal{L}_i \tilde{u}_0 = \mathcal{L}_i^0 \tilde{u}_0 + \mathcal{O}(\delta_i^2) = \mathcal{L}_i^0 u_{0i} + \mathcal{O}(\delta_i^2) = f_i + \mathcal{O}(\delta_i^2), \quad i = 1, 2. \quad (11)$$

Define the error $e = u - \tilde{u}_0$. From (3) and (11), it follows that

$$\mathcal{L}_i e = \mathcal{L}_i(u - \tilde{u}_0) = \mathcal{O}(\delta_i^2), \quad x \in \Omega_i. \quad (12)$$

On the Dirichlet region \mathcal{I}_i^D , the Taylor remainder estimate gives

$$\|e\|_{\infty, \mathcal{I}_i^D} \leq \frac{\delta_i^4}{24} \|\partial_x^4 u_{0i}\|_{\infty, \mathcal{I}_i^D}. \quad (13)$$

By Lemma 2.1, and the construction of \tilde{u}_0 , the flux error satisfies

$$\mathcal{F}(e_1, e_2) = \mathcal{F}(u_1, u_2) - \mathcal{F}(\tilde{u}_{01}, \tilde{u}_{02}) = \psi - \left(\sigma_1 \tilde{u}'_{01}(\alpha) - \sigma_2 \tilde{u}'_{02}(\alpha) + \mathcal{O}(\max(\delta_1^2, \delta_2^2)) \right). \quad (14)$$

Since $\tilde{u}'_{0i}(\alpha) = u'_{0i}(\alpha) + \mathcal{O}(\delta_i^2)$ and $\sigma_1 u'_{01}(\alpha) - \sigma_2 u'_{02}(\alpha) = \psi$, it is conclude that

$$\|\mathcal{F}(e_1, e_2)\|_{\infty, \Gamma} = \mathcal{O}(\max(\delta_1^2, \delta_2^2)).$$

Applying the a priori estimate from Theorem 2.2 yields

$$\|e\|_{\infty, \Omega_i} \leq \left(\max_i \|e\|_{\infty, \mathcal{I}_i^D} + \max_i \|\mathcal{L}_i e\|_{\infty, \Omega_i} + \|\mathcal{F}(e_1, e_2)\|_{\infty, \Gamma} \right).$$

Substituting the bounds in (12) - (14) into the above inequality gives

$$\|e\|_{\infty, \Omega_1 \cup \Omega_2} \leq C \max(\delta_1^2, \delta_2^2).$$

Finally, since $\tilde{u}_0 = u_0$ on $\Omega_1 \cup \Omega_2$, the triangle inequality implies

$$\|u - u_0\|_{\infty, \Omega_1 \cup \Omega_2} \leq \|e\|_{\infty, \Omega_1 \cup \Omega_2} + \|\tilde{u}_0 - u_0\|_{\infty, \Omega_1 \cup \Omega_2} \leq C \max(\delta_1^2, \delta_2^2),$$

which completes the proof. \square

Remark 2.1. If the Dirichlet boundary conditions for the nonlocal problem are prescribed directly as $u_1 = g_{01}$ on \mathcal{I}_1^D , and $u_2 = g_{02}$ on \mathcal{I}_2^D , where g_{01} are taken from the local problem, then the convergence order in Theorem 2.3 reduces to $\max(\delta_1, \delta_2)$. This is due to the mismatch between the local boundary data and the nonlocal extension, which introduces a first-order error in the boundary region.

3. Unfitted finite element method for nonlocal interface problem

This section presents the finite element discretization of the nonlocal interface problem (3)-(4). In contrast to approaches that align element boundaries with the interface Γ_0 to capture flux jumps, an unfitted methodology is adopted. The scheme employs discontinuous piecewise polynomial finite element spaces on a uniform background grid, thereby eliminating any dependence of the discretization on the interface location.

3.1. Weak formulation

The solution and test functions are defined piecewise as follows

$$u = \begin{cases} u_1 & \text{in } \Omega_1 \cup \mathcal{I}_1, \\ u_2 & \text{in } \Omega_2 \cup \mathcal{I}_2, \end{cases} \quad v = \begin{cases} v_1 & \text{in } \Omega_1 \cup \mathcal{I}_1, \\ v_2 & \text{in } \Omega_2 \cup \mathcal{I}_2. \end{cases}$$

The *nonlocal energy norm* $\|\cdot\|_{\delta_i} := \sqrt{(u, u)_{\delta_i}}$ is induced by inner product

$$(u, v)_{\delta_i} := \frac{1}{2} \int_{\Omega_i \cup \mathcal{I}_i^D} \int_{\Omega_i \cup \mathcal{I}_i^D} [u_i(x) - u_i(y)][v_i(x) - v_i(y)] \gamma_{\delta_i}(x, y) dy dx.$$

To account for coupling effects across the interface Γ , an additional inner product is introduced

$$(u, v)_{\Gamma} := \frac{1}{2} \sum_{i=1}^2 \int_{\mathcal{I}_i^J} \int_{\mathcal{I}_i^J} [u_i(x) - u_i(y)][v_i(x) - v_i(y)] \gamma_{\delta_i}(x, y) dy dx \\ + \int_{\mathcal{I}_2^J} \int_{\Omega_2^J} [u_2(x) - u_2(y)][v_2(x) - v_2(y)] \gamma_{\delta_2}(x, y) dy dx,$$

with the corresponding norm $\|u\|_{\Gamma} := \sqrt{(u, u)_{\Gamma}}$. The global nonlocal energy norm is then defined as $\|u\|_{\delta}^2 := \|u\|_{\delta_1}^2 + \|u\|_{\delta_2}^2 + \|u\|_{\Gamma}^2$. The energy space is given by

$$V_{\delta} := \{v \in L^2(\Omega \cup \mathcal{I}^D) : \|u\|_{\delta} < \infty, v_i = 0 \text{ in } \mathcal{I}_i^D, v_1 = v_2 \text{ in } \Gamma\},$$

and its dual space is denoted by V'_{δ} . The weak formulation of (3)-(4) reads: given $f \in V'_{\delta}$ and $\psi \in V'_{\delta}$, find $u \in V_{\delta}$ such that

$$a(u_1, u_2, v_1, v_2) = l(v_1, v_2), \quad \text{for all } v \in V_{\delta}, \quad (15)$$

where the bilinear and linear forms are respectively defined as

$$a(u_1, u_2, v_1, v_2) = \frac{1}{2} \sum_{i=1}^2 \int_{\Omega_i \cup \mathcal{I}_i^D} \int_{\Omega_i \cup \mathcal{I}_i^D} (u_i(x) - u_i(y))(v_i(x) - v_i(y)) \gamma_{\delta_i}(x, y) dy dx \\ + \frac{1}{2} \sum_{i=1}^2 \int_{\mathcal{I}_i^J} \int_{\mathcal{I}_i^J} (u_i(x) - u_i(y))(v_i(x) - v_i(y)) \gamma_{\delta_i}(x, y) dy dx \\ + \int_{\mathcal{I}_2^J} \int_{\Omega_2^J} (u_2(x) - u_2(y))(v_2(x) - v_2(y)) \gamma_{\delta_2}(x, y) dy dx, \\ l(v_1, v_2) = \sum_{i=1}^2 \int_{\Omega_i} f_i(x) v_i(x) dx + \int_{\mathcal{I}_2^J} \psi_1(x) v_1(x) dx + \int_{\mathcal{I}_1^J} \psi_2(x) v_2(x) dx.$$

The well-posedness of the weak formulation (15) has been established in [8].

3.2. Unfitted finite element discretization

A uniform partition \mathcal{T}^h of the computational domain $\Omega \cup \mathcal{I}^D$ is constructed, with nodes distributed as $a - \delta_1 = x_0 < \dots < x_{M_1-1} < a = x_{M_1} < \dots < x_{M_1+N} = b < \dots < x_{N+M_1+M_2} = b + \delta_2$. Notably, the interface point $\alpha \in (a, b)$ is not required to align with any grid nodes. The mesh parameter h denotes the length of uniform subinterval $K = (x_j, x_{j+1})$, for $j = 0, 1, \dots, N + M_1 + M_2 - 1$. To handle the nonlocal interface $\Gamma = (\alpha - \delta_2, \alpha + \delta_1)$, elements are classified as follows

- Interface-intersecting elements: $\mathcal{T}_\Gamma^h = \{T \in \mathcal{T}^h : T \cap \Gamma \neq \emptyset\}$,
- Nonlocal interaction elements: $\mathcal{T}_{i,J}^h = \{T \in \mathcal{T}^h : T \cap \mathcal{I}_i^J \neq \emptyset\}$, $i = 1, 2$, $\mathcal{T}_{\Omega_2^J}^h = \{T \in \mathcal{T}^h : T \cap \Omega_2^J \neq \emptyset\}$,
- Subdomain elements: $\mathcal{T}_i^h = \{T \in \mathcal{T}^h : \overline{T} \cap (\Omega_i \cup \mathcal{I}_i^D) \neq \emptyset\}$, $i = 1, 2$.

The corresponding finite element spaces are defined as

$$V_i^h = \{v \in L^2(\Omega_i \cup \mathcal{I}_i^D) : v|_K \in \mathbb{P}^k(K), \forall K \in \mathcal{T}_i^h\}, \quad V^h = V_1^h \times V_2^h,$$

with the constrained space $V^{0,h} = \{v^h \in V^h : v^h|_{\mathcal{I}^D} = 0\}$, where $\mathbb{P}^k(K)$ denotes by the space of polynomials of degree at most k on element K . The discrete weak formulation seeks $u^h = (u_1^h, u_2^h) \in V^h$ such that

$$a(u_1^h, u_2^h, v_1^h, v_2^h) = l(v_1^h, v_2^h), \quad \forall v^h \in V^{0,h}. \quad (16)$$

3.3. Implementation

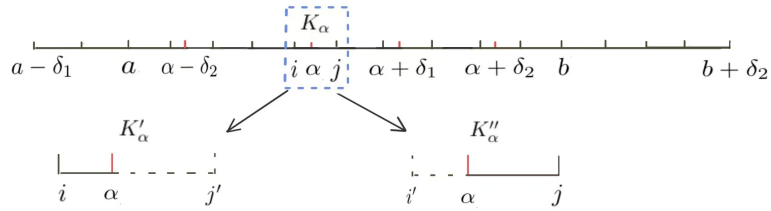


Figure 1: Schematic of the non-interface-conforming uniform mesh

For illustration, the lowest-order case is considered, using piecewise-linear basis functions. The algorithm first identifies the element K_α intersected by the local interface Γ_0 . This element is then subdivided into a left sub-interval K'_α and a right sub-interval K''_α . On K'_α , a virtual nodes j' is introduced on the far side of Γ_0 , while on K''_α , a virtual nodes i' is placed on the opposite side (see Figure 1). These nodes serve as algebraic placeholders: they coincide geometrically with Γ_0 , but are not conventional finite element vertices. Their purpose is to decouple the discrete function spaces on Ω_1 and Ω_2 while preserving the physical geometry. A consistency check guarantees that no spurious duplication occurs at element

boundaries. Upon completion, two independent meshes are obtained: one for Ω_1 and another for Ω_2 , each containing interface-adjacent elements that are geometrically coincident but topologically distinct.

For the finite element discretization, the solution u^h and test functions v^h are expanded in the piecewise linear basis functions $\{\phi_m\}_{m=1}^{M_d}$, where the index set M_h includes all physical and virtual degrees of freedom. Substitution into the weak formulation (16) yields the linear system

$$\mathbb{A}\mathbf{U}_h = \mathbf{b},$$

where \mathbf{U}_h is the vector of nodal unknowns, \mathbb{A} is the global stiffness matrix, and \mathbf{b} is the load vector. To streamline assembly, the matrix is decomposed additively as

$$\mathbb{A} = \mathbb{A}_\Omega + \mathbb{A}_\Gamma.$$

Here, \mathbb{A}_Ω collects standard nonlocal element contributions over \mathcal{T}_i^h , while \mathbb{A}_Γ encodes the interface terms integrated over $\mathcal{T}_\Gamma^h \cup \mathcal{T}_{\Omega_2, J}^h$. In one dimension, the computation of \mathbb{A}_Γ is exact and efficient: a simple affine mapping to the reference element reduces all interface integrals to closed-form expressions. Although the virtual nodes are essential for embedding the jump conditions directly into the weak form, they are purely algebraic artifacts and do not belong to the physical domain Ω . This approach captures discontinuities across the interface without body-fitted meshing, underscoring the method's robustness for nonlocal interface problems.

3.4. Error estimate for the unfitted FEM

A priori error estimates are now established for the unfitted finite element discretization of nonlocal interface problems, quantifying approximation errors in both energy and L^2 norms. The analysis relies on two key lemmas, whose proofs are provided in Appendix 6.2.

Lemma 3.1. Suppose the kernel family $\{\gamma_{\delta_i}\}$ satisfies (1), (2) and (9). Then there exists a constant $C > 0$ such that for all piecewise continuous bounded functions $v = (v_1, v_2)$ with $v_i \in C_b(\Omega_i \cup \mathcal{I}_i^D)$, the following bound holds

$$\|v\|_\delta \leq C \max\{\delta_1^{-1}, \delta_2^{-1}\} \left(\|v\|_{\infty, \Omega_1 \cup \Omega_2} + \|v\|_{\infty, \mathcal{I}_1^D \cup \mathcal{I}_2^D} \right).$$

Lemma 3.2. Under the same kernel assumptions, there exist constants $C_1, C_2 > 0$, depending only on Ω and γ_i , such that for all $v \in V^0 = \{v \in L^2(\Omega_1 \cup \Omega_2) : v|_{\mathcal{I}_i^D} = 0\}$,

$$C_1 \|v\|_{L^2(\Omega_1 \cup \Omega_2)} \leq \|v\|_\delta \leq C_2 \max\{\delta_1^{-1}, \delta_2^{-1}\} \|v\|_{L^2(\Omega_1 \cup \Omega_2)}. \quad (17)$$

The main convergence result for the unfitted FEM is now presented.

Theorem 3.1. Under the assumptions of Theorem 2.3, if \tilde{u}_0 is a $C_b^{\max(4, k+1)}(\Omega_1 \cup \Omega_2)$ extension of u_0 , and u^h is the finite element solution in V^h with k -th degree Lagrange interpolation of boundary data g_i^h , then there exists a constant $C > 0$, independent of δ_1, δ_2 and h , such that

$$\|u - u^h\|_\delta \leq C \max\{\delta_1^{-1}, \delta_2^{-1}\} h^{k+1}, \quad (18)$$

$$\|u - u^h\|_{L^2(\Omega_1 \cup \Omega_2)} \leq C \max\{\delta_1^{-1}, \delta_2^{-1}\} h^{k+1}. \quad (19)$$

Proof. Let $u^* = (u_1^*, u_2^*) \in V^h$ be a projection of the exact nonlocal solution u onto the finite element space, satisfying

$$\mathcal{L}_i u_i^* = f_i, \quad \text{in } \Omega_i, \quad u_i^* = g_i^h, \quad \text{on } \mathcal{I}_i^D, \quad (20)$$

and the jump conditions

$$[[u^*]] = 0, \quad \mathcal{F}(u_1^*, u_2^*) = \psi(x), \quad \text{on } \Gamma. \quad (21)$$

From (3) and (20), the residual satisfies

$$\mathcal{L}_i(u_i - u_i^*) = 0, \quad x \in \Omega_i.$$

The interface conditions (4) and (21) imply

$$\mathcal{F}(u_i - u_i^*, u_i - u_i^*) = 0, \quad \text{in } \Gamma.$$

Applying the nonlocal maximum principle (Theorem 2.1) yields

$$\begin{aligned} \|u - u^*\|_{\infty, \Omega_1 \cup \Omega_2} &\leq \|u - u^*\|_{\infty, \mathcal{I}_1^D \cup \mathcal{I}_2^D} + C \|\mathcal{L}(u - u^*)\|_{\infty, \Omega_1 \cup \Omega_2} + \|\mathcal{F}(u_1 - u_1^*, u_2 - u_2^*)\|_{\infty, \Gamma} \\ &\leq C_I h^{k+1} \|u\|_{C_b^{k+1}(\mathcal{I}_1^D \cup \mathcal{I}_2^D)}. \end{aligned} \quad (22)$$

Lemma 3.1 then gives

$$\|u - u^*\|_\delta \leq C \max\{\delta_1^{-1}, \delta_2^{-1}\} h^{k+1} \|u\|_{C_b^{k+1}(\mathcal{I}_1^D \cup \mathcal{I}_2^D)}.$$

Now consider the discrete error $u^* - u^h$. By Galerkin orthogonality of (16),

$$a(u^* - u^h, v^h) = 0, \quad \forall v^h \in V^{0,h}. \quad (23)$$

Let $I_h \tilde{u}_0$ be the piecewise k -degree polynomial interpolation of \tilde{u}_0 . Standard interpolation theory gives

$$\|\tilde{u}_0 - I_h \tilde{u}_0\|_\delta \leq C \max\{\delta_1^{-1}, \delta_2^{-1}\} \|\tilde{u}_0 - I_h \tilde{u}_0\|_{\infty, \Omega_1 \cup \Omega_2} \leq C \max\{\delta_1^{-1}, \delta_2^{-1}\} \|\tilde{u}_0\|_{C_b^{k+1}(\Omega_1 \cup \Omega_2)}.$$

Choosing $v^h = I_h \tilde{u}_0 - u^h$ in (23) and using the coercivity and continuity of $a(\cdot, \cdot)$ leads to

$$\|u^* - u^h\|_\delta \leq \|u^* - I_h \tilde{u}_0\|_\delta.$$

By the triangle inequality and Lemma 3.1,

$$\begin{aligned} \|u^* - I_h \tilde{u}_0\|_\delta &\leq \|u^* - u\|_\delta + \|u - \tilde{u}_0\|_\delta + \|\tilde{u}_0 - I_h \tilde{u}_0\|_\delta \\ &\leq C \max\{\delta_1^{-1}, \delta_2^{-1}\} h^{k+1} + C \max\{\delta_1, \delta_2\}. \end{aligned}$$

For $h \leq \min\{\delta_1, \delta_2\}$, the terms involving h^{k+1} dominate, yielding

$$\|u^* - u^h\|_\delta \leq C \max\{\delta_1^{-1}, \delta_2^{-1}\} h^{k+1}.$$

Thus,

$$\|u - u^h\|_\delta \leq \|u - u^*\|_\delta + \|u^* - u^h\|_\delta \leq C \max\{\delta_1^{-1}, \delta_2^{-1}\} h^{k+1},$$

which proves (18). For the L^2 estimate, since $u^* - u^h \in V^0$, Lemma 3.2 gives

$$\|u^* - u^h\|_{L^2(\Omega_1 \cup \Omega_2)} \lesssim \|u^* - u^h\|_\delta \lesssim \max\{\delta_1^{-1}, \delta_2^{-1}\} h^{k+1}.$$

Applying the triangle inequality again yields

$$\|u - u^h\|_{L^2(\Omega_1 \cup \Omega_2)} \leq \|u - u^*\|_{L^2(\Omega_1 \cup \Omega_2)} + \|u^* - u^h\|_{L^2(\Omega_1 \cup \Omega_2)} \leq C \max\{\delta_1^{-1}, \delta_2^{-1}\} h^{k+1},$$

which completes the proof of (19). \square

Remark 3.1. The convergence rates stated in (19) may be suboptimal, as they rely on the generic inequality (17). However, numerical experiments in Section 4 indicate that the discrete L_2 error converges one order higher than the energy error, suggesting that the theoretical bounds can be sharpened. The current estimates are therefore regarded as a baseline.

3.5. Error estimates between nonlocal discrete solutions and local exact solution

Combining the results of Sections 2 and 3, we establish the convergence of the nonlocal finite element solutions to the local limit solution.

Theorem 3.2. Suppose the kernel family $\{\gamma_{\delta_i}\}$ satisfies (1), (2) and (9). Let $C_b^{\max(4, k+1)}(\Omega_1 \cup \Omega_2)$ be the solution to the local interface problem (6)–(7), and let \tilde{u}_0 be a C^4 extension of u_0 to $\Omega \cup \mathcal{I}^D$ such that $\tilde{u}_0|_{\mathcal{I}^D} = g_i$. Then for the unfitted FEM approximation u^h , there exists constant $C > 0$, independent of δ_1, δ_2 and h , such that

$$\|\tilde{u}_0 - u^h\|_\delta \leq C \max\{\delta_1^{-1}, \delta_2^{-1}\} h^{k+1}, \quad (24)$$

$$\|\tilde{u}_0 - u^h\|_{L^2(\Omega_1 \cup \Omega_2)} \leq C \max\{\delta_1^{-1}, \delta_2^{-1}\} h^{k+1}. \quad (25)$$

Proof. Let u denote the exact nonlocal solution to (3)–(4). Splitting the error gives

$$\|\tilde{u}_0 - u^h\|_\delta \leq \|\tilde{u}_0 - u\|_\delta + \|u - u^h\|_\delta. \quad (26)$$

From Theorem 2.3 and Lemma 3.1,

$$\|\tilde{u}_0 - u\|_\delta \leq C \max\{\delta_1^{-1}, \delta_2^{-1}\} \|\tilde{u}_0 - u\|_\infty \leq C \max\{\delta_1, \delta_2\}. \quad (27)$$

Theorem 3.1 yields

$$\|u - u^h\|_\delta \leq C \max\{\delta_1^{-1}, \delta_2^{-1}\} h^{k+1}. \quad (28)$$

For $h \leq \min(\delta_1, \delta_2)$, the discrete error dominates, yielding (24). The L^2 estimate follows similarly using Lemma 3.2 and noting $\|u_0 - \tilde{u}_0\|_{L^2} = 0$ on Ω . \square

4. Numerical examples

This section presents numerical experiments to validate the theoretical predictions and to evaluate the performance of the unfitted finite-element method for nonlocal elliptic interface problems. Three representative configurations are examined: a solution continuous across the interface (Example 4.1), a solution exhibiting an interfacial jump (Example 4.2), and a multi-interface configuration (Example 4.3). The computed errors confirm the convergence rates asserted in Theorem 3.2 and demonstrate that the method resolves solution discontinuities with high fidelity.

Example 4.1. The domain is taken as $\Omega = (0, 1)$ with the interface point at $\alpha = \pi/6$. For nonlocal interaction horizons parameters δ_1 and δ_2 , the kernel functions are selected as $\gamma_{\delta_i}(x, y) = 6\delta_i^{-4}(\delta_i - |x - y|)$, $i = 1, 2$. The exact solutions $u_1(x)$ and $u_2(x)$ are constructed as

$$u_1(x) = \begin{cases} 0 & -\delta_1 < x \leq 0, \\ \sin x & 0 < x \leq \alpha, \\ 3/2 - 2 \sin x & \alpha < x \leq \alpha + \delta_1, \end{cases} \quad u_2(x) = \begin{cases} \sin x & \alpha - \delta_2 < x \leq \alpha, \\ 3/2 - 2 \sin x & \alpha < x < 1, \\ 3/2 - 2 \sin 1 & 1 \leq x < 1 + \delta_2. \end{cases}$$

The solution is continuous across the interface, satisfying $u_1(\alpha) = u_2(\alpha)$.

The left panel of Figure 2 presents the numerical solution obtained with polynomial degree $k = 2$. The approximation agrees with the exact solution to graphical accuracy, including at the interface.

Table 1 lists the errors in L^2 and energy norms by fixed δ_i and varying h , showing optimal $k + 1$ -order convergence for piecewise polynomials of degree k . Table 2 shows the δ -convergence where $\delta = Mh$ is fixed while h is refined. The results indicate k -order convergence in the energy norm and $k + 1$ -order convergence in the L^2 norm, suggesting potential for improved theoretical estimates.

Table 1: Error norms and convergence rates for $\delta_1 = 1/4$ and $\delta_2 = 1/2$

	$k = 1$		$k = 2$		$k = 3$	
h	$\ u - u^h\ _\delta$	$\ u - u^h\ _{L^2}$	$\ u - u^h\ _\delta$	$\ u - u^h\ _{L^2}$	$\ u - u^h\ _\delta$	$\ u - u^h\ _{L^2}$
2^{-2}	1.50e-02	5.00e-03	5.43e-04	1.46e-04	3.91e-06	2.15e-06
2^{-3}	4.10e-03[1.87]	1.30e-03[1.94]	7.39e-05[2.88]	1.86e-05[2.97]	2.65e-07[3.89]	1.37e-07[3.96]
2^{-4}	1.10e-03[1.90]	3.16e-04[2.04]	9.57e-06[2.95]	2.39e-06[2.96]	1.70e-08[3.96]	8.76e-09[3.97]
2^{-5}	2.82e-04[1.96]	7.94e-05[1.99]	1.23e-06[2.96]	3.06e-07[2.96]	1.10e-09[3.96]	5.55e-10[3.98]

Table 2: Error norms and convergence rates for $\delta_1 = 2h$ and $\delta_2 = 4h$

	$k = 1$		$k = 2$		$k = 3$	
h	$\ u - u^h\ _\delta$	$\ u - u^h\ _{L^2}$	$\ u - u^h\ _\delta$	$\ u - u^h\ _{L^2}$	$\ u - u^h\ _\delta$	$\ u - u^h\ _{L^2}$
2^{-3}	4.10e-03	1.30e-03	7.39e-05	1.86e-05	2.65e-07	1.37e-07
2^{-4}	1.40e-03[1.55]	3.13e-04[2.05]	1.89e-05[1.96]	2.38e-06[2.96]	3.17e-08[3.06]	8.72e-09[3.98]
2^{-5}	5.12e-04[1.45]	7.84e-05[2.00]	4.84e-06[1.96]	3.05e-07[2.96]	3.93e-09[3.01]	5.54e-10[3.98]
2^{-6}	1.77e-04[1.53]	1.96e-05[2.00]	1.22e-06[1.99]	3.84e-08[2.99]	4.85e-10[3.02]	3.46e-11[4.00]

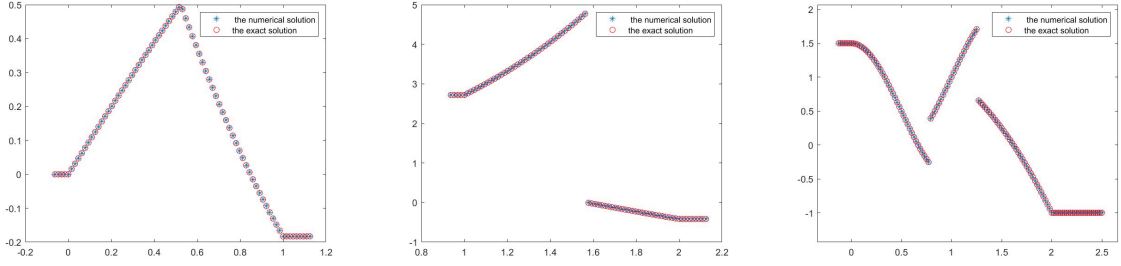


Figure 2: The numerical solution of Example 4.1-4.3.

Example 4.2. This example tests the case with a solution discontinuity at the interface in $\Omega = (1, 2)$ with $\alpha = \pi/2$. The kernel functions are $\gamma_{\delta_i} = 3\delta_i^{-3}/2$, $i = 1, 2$. The exact solutions with a jump at α are

$$u_1(x) = \begin{cases} e & 1 - \delta_1 < x \leq 1 \\ e^x & 1 < x \leq \alpha \\ \cos x & \alpha < x \leq \alpha + \delta_1, \end{cases} \quad u_2(x) = \begin{cases} e^x & \alpha - \delta_2 < x \leq \alpha \\ \cos x & \alpha < x < 2 \\ \cos 2 & 2 \leq x < 2 + \delta_2. \end{cases}$$

Tables 3 and 4 illustrate that the method accurately captures the jump condition, handling discontinuities without loss of accuracy. Similar to Example 4.1, the convergence rates match the theoretical expectations, with L^2 errors again exhibiting higher-order convergence. Figure 2 (middle) compares the numerical solutions for polynomial degrees $k = 2$ with the exact solution, confirming the method's sharp resolution of the discontinuity at the interface.

Table 3: Error norms and convergence rates for $\delta_1 = 1/4$ and $\delta_2 = 1/2$

	$k = 1$		$k = 2$		$k = 3$	
h	$\ u - u^h\ _\delta$	$\ u - u^h\ _{L^2}$	$\ u - u^h\ _\delta$	$\ u - u^h\ _{L^2}$	$\ u - u^h\ _\delta$	$\ u - u^h\ _{L^2}$
2^{-2}	4.32e-02	1.33e-02	1.30e-03	3.47e-04	1.43e-05	6.07e-06
2^{-3}	1.04e-02[2.05]	3.30e-03[2.01]	1.65e-04[2.98]	4.29e-05[3.02]	8.94e-07[4.00]	3.73e-07[4.03]
2^{-4}	2.80e-03[1.89]	9.13e-04[1.85]	2.24e-05[2.88]	5.85e-06[2.88]	6.05e-08[3.88]	2.55e-08[3.87]
2^{-5}	6.92e-04[2.02]	2.27e-04[2.01]	2.80e-06[3.00]	7.27e-07[3.01]	3.79e-09[4.00]	1.58e-09[4.01]

Table 4: Error norms and convergence rates for $\delta_1 = 2h$ and $\delta_2 = 4h$

	$k = 1$		$k = 2$		$k = 3$	
h	$\ u - u^h\ _\delta$	$\ u - u^h\ _{L^2}$	$\ u - u^h\ _\delta$	$\ u - u^h\ _{L^2}$	$\ u - u^h\ _\delta$	$\ u - u^h\ _{L^2}$
2^{-3}	1.04e-02	3.30e-03	4.41e-08	4.29e-05	8.94e-07	3.73e-07
2^{-4}	4.00e-03[1.38]	9.04e-04[1.87]	4.51e-05[1.87]	5.85e-06[2.88]	1.19e-07[2.92]	2.55e-08[3.87]
2^{-5}	1.40e-03[1.51]	2.24e-04[2.01]	1.13e-05[1.99]	7.26e-07[3.01]	1.47e-08[3.02]	1.59e-09[4.00]
2^{-6}	4.98e-04[1.49]	5.61e-05[2.00]	2.84e-06[2.00]	9.03e-08[3.01]	1.82e-09[3.01]	9.78e-11[4.02]

Example 4.3. The domain $\Omega = (0, 2)$ is considered with interfaces at $\alpha_1 = \pi/4$ and $\alpha_2 = 2\pi/5$. For given $\delta_1, \delta_2, \delta_3$, the kernel functions are defined as

$$\gamma_{\delta_i} = \frac{12}{\delta_i^5}(\delta_i^2 - |x - y|^2), \quad i = 1, 2, 3.$$

The exact solutions $u_1(x)$, $u_2(x)$ and $u_3(x)$ are designed to exhibit jumps at both interfaces

$$u_1(x) = \begin{cases} \frac{1}{2} & -\delta_1 < x \leq 0, \\ \frac{1}{2} \cos(\pi x) & 0 < x \leq \alpha_1 \\ 1 - \sin(\pi x) & \alpha_1 < x \leq \alpha_1 + \delta_1, \end{cases}$$

$$u_2(x) = \begin{cases} \frac{1}{2} \cos(\pi x) & \alpha_1 - \delta_2 < x \leq \alpha_1, \\ 1 - \sin(\pi x) & \alpha_1 < x \leq \alpha_2 \\ x(1-x) + 1 & \alpha_2 < x < \alpha_2 + \delta_2. \end{cases} \quad u_3(x) = \begin{cases} 1 - \sin(\pi x) & \alpha_2 - \delta_2 < x \leq \alpha_2, \\ x(1-x) + 1 & \alpha_2 < x < 2 \\ -1 & 2 \leq x < \alpha_2/2 + \delta_2. \end{cases}$$

Tables 5 and 6 present the error norms and convergence rates for fixed horizons and horizon-to-mesh ratios, respectively. The results confirm the theoretical estimates, demonstrating optimal convergence rates in both the energy and L^2 norms. Figure 2 (right) shows that the method accurately resolves discontinuities at multiple interfaces, further validating its robustness for problems involving complex interfacial geometries.

Table 5: Errors norms and convergence rates for $\delta_1 = 1/8$, $\delta_2 = 1/4$ and $\delta_3 = 1/2$

	$k = 1$		$k = 2$		$k = 3$	
h	$\ u - u^h\ _\delta$	$\ u - u^h\ _{L^2}$	$\ u - u^h\ _\delta$	$\ u - u^h\ _{L^2}$	$\ u - u^h\ _\delta$	$\ u - u^h\ _{L^2}$
2^{-3}	8.00e-02	7.50e-03	7.00e-03	4.61e-04	8.99e-05	8.39e-06
2^{-4}	2.03e-02[1.98]	2.00e-03[1.91]	8.67e-04[3.01]	5.82e-05[2.99]	5.50e-06[4.03]	5.35e-07[3.97]
2^{-5}	5.10e-03[1.99]	5.06e-04[1.98]	1.08e-04[3.01]	7.28e-06[3.00]	3.39e-07[4.02]	3.39e-08[3.98]
2^{-6}	1.20e-03[2.09]	1.39e-04[1.86]	1.33e-05[3.02]	9.04e-07[3.01]	2.10e-08[4.01]	2.12e-09[4.00]

Table 6: Errors norms and convergence rates for $\delta_1 = h$, $\delta_2 = 2h$ and $\delta_3 = 3h$

	$k = 1$		$k = 2$		$k = 3$	
h	$\ u - u^h\ _\delta$	$\ u - u^h\ _{L^2}$	$\ u - u^h\ _\delta$	$\ u - u^h\ _{L^2}$	$\ u - u^h\ _\delta$	$\ u - u^h\ _{L^2}$
2^{-3}	8.02e-02	7.40e-03	7.00e-03	4.61e-04	9.00e-05	8.38e-06
2^{-4}	2.75e-02[1.54]	1.90e-03[1.96]	1.80e-03[1.96]	5.96e-05[2.95]	1.12e-05[3.01]	5.36e-07[3.97]
2^{-5}	9.80e-03[1.49]	4.96e-04[1.94]	4.54e-04[1.99]	7.89e-06[2.92]	1.42e-06[2.98]	3.49e-08[3.94]
2^{-6}	3.50e-03[1.49]	1.27e-04[1.97]	1.14e-04[1.99]	9.71e-07[3.02]	1.77e-07[3.00]	2.40e-09[3.86]

The numerical results validate the theoretical error estimates even for solutions discontinuous across the interface. In all case, the discrete L^2 error converges at an order higher than predicted, indicating that the current theoretical bounds can be improved. The method's robustness with respect to interfacial jumps underscores its applicability to practical problems involving material discontinuities or sharp phase boundaries.

5. Conclusion

This paper has introduced an AC unfitted finite element framework for one-dimensional nonlocal elliptic interface problems. The analysis establishes second-order convergence of the nonlocal solution to the local limit as the horizon parameters tend to zero. By incorporating nonlocal jump conditions directly into the weak formulation via a Nitsche-type approach, the method accommodates solution discontinuities without requiring mesh conformity to the interface. Optimal convergence rates of order $(k + 1)$ in both the energy and L^2 norms are rigorously proven for piecewise polynomial approximations of degree k .

Numerical experiments demonstrate the robustness of the scheme for both continuous and discontinuous interfacial solutions, confirming the theoretical findings. The proposed asymptotically compatible unfitted framework offers a practical and efficient foundation for addressing more complex problems in computational mechanics. A natural and critical extension of this work is to higher spatial dimensions, which would significantly broaden its applicability to realistic engineering problems. Future research will also focus on time-dependent nonlocal interface problems, such as dynamic fracture and elastodynamics with evolving micro-cracks. The mathematical analysis and numerical tools developed in this one-dimensional study serve as a cornerstone for these ambitious extensions.

6. Appendix

This appendix provides detailed proofs of the key lemmas and theorems. Section 6.1 contains the proof of Lemma 2.1, which establishes the local limit of the interface flux operator. Section 6.2 presents the proofs of Lemmas 3.1 and 3.2, which are essential to the error analysis of the unfitted finite element scheme.

6.1. Proof of Lemma 2.1

The nonlocal flux operator $\mathcal{F}(\hat{u}_1, \hat{u}_2)$ is analyzed by decomposing its action as follows

$$(\mathcal{F}(\hat{u}_1, \hat{u}_2), v)_{\mathcal{I}_2^J} + (\mathcal{F}(\hat{u}_1, \hat{u}_2), v)_{\mathcal{I}_1^J} = \mathcal{I}_1 + \mathcal{I}_2 + \mathcal{I}_3 + \mathcal{I}_4 + \mathcal{I}_5,$$

where the terms are defined by

$$\begin{aligned} \mathcal{I}_1 &= \int_{\alpha-\delta_2}^{\alpha} \int_{\alpha+\delta_1}^{\alpha+\delta_2} [\hat{u}_2(x) - \hat{u}_2(y)] \gamma_{\delta_2}(x, y) v(x) dy dx, \quad \mathcal{I}_2 = \frac{1}{2} \int_{\alpha-\delta_2}^{\alpha} \int_{\alpha}^{\alpha+\delta_1} [\hat{u}_1(x) - \hat{u}_1(y)] \gamma_{\delta_2}(x, y) v(x) dy dx, \\ \mathcal{I}_3 &= -\frac{1}{2} \int_{\alpha-\delta_2}^{\alpha} \int_{\alpha}^{\alpha+\delta_1} [\hat{u}_1(x) - \hat{u}_1(y)] \gamma_{\delta_1}(x, y) v(x) dy dx, \quad \mathcal{I}_4 = \frac{1}{2} \int_{\alpha}^{\alpha+\delta_1} \int_{\alpha-\delta_2}^{\alpha} [\hat{u}_2(x) - \hat{u}_2(y)] \gamma_{\delta_1}(x, y) v(x) dy dx, \\ \mathcal{I}_5 &= -\frac{1}{2} \int_{\alpha}^{\alpha+\delta_1} \int_{\alpha-\delta_2}^{\alpha} [\hat{u}_2(x) - \hat{u}_2(y)] \gamma_{\delta_2}(x, y) v(x) dy dx. \end{aligned}$$

For \mathcal{I}_1 , the coordinate transformations $x = \alpha - t\delta_2$, $y = \alpha + s\delta_2$ with $t \in [0, 1]$, $s \in [\delta_1/\delta_2, 1]$ yield

$$\mathcal{I}_1 = \frac{1}{\delta_2} \int_{t=0}^1 \int_{s=\delta_1/\delta_2}^1 [\hat{u}_2(\alpha - t\delta_2) - \hat{u}_2(\alpha + s\delta_2)] \gamma_2(t + s) v(\alpha - t\delta_2) ds dt.$$

Taylor expansions about α give

$$\begin{aligned}\hat{u}_2(\alpha - t\delta_2) &= \hat{u}_2(\alpha) - \hat{u}'_2(\alpha)t\delta_2 + \frac{1}{2}\hat{u}''_2(\alpha)t^2\delta_2^2 + \mathcal{O}(\delta_2^3), \\ \hat{u}_2(\alpha + s\delta_2) &= \hat{u}_2(\alpha) + \hat{u}'_2(\alpha)s\delta_2 + \frac{1}{2}\hat{u}''_2(\alpha)s^2\delta_2^2 + \mathcal{O}(\delta_2^3), \\ v(\alpha - t\delta_2) &= v(\alpha) + \mathcal{O}(\delta_2).\end{aligned}$$

Substituting into \mathcal{I}_1 leads to

$$\mathcal{I}_1 = -\hat{u}'_2(\alpha)v(\alpha)\mathcal{I}_1^1 + \frac{1}{2}\delta_2\hat{u}''_2(\alpha)v(\alpha)\mathcal{I}_1^2 + \mathcal{O}(\delta_2^2),$$

where

$$\mathcal{I}_1^1 = \int_{t=0}^1 \int_{s=\delta_1/\delta_2}^1 (t+s)\gamma_2(t+s) ds dt, \quad \mathcal{I}_1^2 = \int_{t=0}^1 \int_{s=\delta_1/\delta_2}^1 (t^2 - s^2)\gamma_2(t+s) ds dt.$$

Similar expressions apply to \mathcal{I}_2 - \mathcal{I}_5 . Combining the terms involving γ_1 -kernel gives

$$\mathcal{I}_3 + \mathcal{I}_4 = \hat{u}'_1(\alpha)v(\alpha)\mathcal{I}_{\sigma_1}^1 + \frac{1}{2}\delta_1\hat{u}''_1(\alpha)v(\alpha)\mathcal{I}_{\sigma_1}^2 + \mathcal{O}(\delta_1^2),$$

with

$$\mathcal{I}_{\sigma_1}^1 = \int_{s=0}^1 \int_{t=0}^{\delta_2/\delta_1} (s+t)\gamma_1(s+t) dt ds, \quad \mathcal{I}_{\sigma_1}^2 = \int_{t=0}^1 \int_{z=t}^{t+\delta_2/\delta_1} (2zt - z^2)\gamma_1(z) dz dt.$$

Similarly, combining the γ_2 -terms yields

$$\mathcal{I}_1 + \mathcal{I}_2 + \mathcal{I}_5 = -\hat{u}'_2(\alpha)v(\alpha)\mathcal{I}_{\sigma_2}^1 + \frac{1}{2}\delta_2\hat{u}''_2(\alpha)v(\alpha)\mathcal{I}_{\sigma_2}^2 + \mathcal{O}(\delta_2^2),$$

where

$$\mathcal{I}_{\sigma_2}^1 = \int_0^1 \int_0^1 (t+s)\gamma_2(t+s) ds dt, \quad \mathcal{I}_{\sigma_2}^2 = \int_{t=0}^1 \int_{z=t}^{t+1} (2zt - z^2)\gamma_2(z) dz dt.$$

Direct calculation shows that $\mathcal{I}_{\sigma_1}^2 = \mathcal{I}_{\sigma_2}^2 = 0$. For $\mathcal{I}_{\sigma_1}^1$,

$$\begin{aligned}\mathcal{I}_{\sigma_1}^1 &= \int_{s=0}^1 \int_{z=s}^{s+\delta_2/\delta_1} z\gamma_1(z) dz ds, \\ &= \int_{z=0}^1 \int_{s=0}^z z\gamma_1(z) ds dz + \int_{z=1}^{\delta_2/\delta_1} \int_{s=0}^1 z\gamma_1(z) ds dz = \int_0^1 z^2\gamma_1(z) dz.\end{aligned}$$

and for $\mathcal{I}_{\sigma_2}^1$,

$$\begin{aligned}\mathcal{I}_{\sigma_2}^1 &= \int_{x=0}^2 \left(\int_{t=\max(0, x-1)}^{\min(1, x)} x\gamma_2(x) dt \right) dx \\ &= \int_{x=0}^1 x^2\gamma_2(x) dx + \int_{x=1}^2 x(2-x)\gamma_2(x) dx = \int_0^1 x^2\gamma_2(x) dx.\end{aligned}$$

Recalling the moment condition (2), it follows that $\mathcal{I}_{\sigma_i}^1 = 2\sigma_i$. Combining all terms gives the desired result

$$\mathcal{F}(\hat{u}_1, \hat{u}_2) = \sigma_1\hat{u}'_1(\alpha) - \sigma_2\hat{u}'_2(\alpha) + \mathcal{O}(\max(\delta_1^2, \delta_2^2)).$$

This completes the proof of Lemma 2.1.

6.2. Proofs of Lemmas 3.1 and 3.2

Proof of Lemmas 3.1. Each component of the energy norm is estimated separately. For $\|v\|_{\delta_i}^2$,

$$\|v\|_{\delta_i}^2 \leq \int_{\Omega_i \cup \mathcal{I}_i^D} \int_{\Omega_i \cup \mathcal{I}_i^D} (v_i^2(x) + v_i^2(y)) \gamma_{\delta_i}(x, y) dy dx = 2 \int_{\Omega_i \cup \mathcal{I}_i^D} v_i^2(x) \left(\int_{\Omega_i \cup \mathcal{I}_i^D} \gamma_{\delta_i}(x, y) dy \right) dx.$$

Using assumption (9) and the boundedness of v_i

$$\|v\|_{\delta_i}^2 \leq 2G(\gamma_{\delta_i}) \left(|\Omega_i| \|v_i\|_{\infty, \Omega_i}^2 + |\mathcal{I}_i^D| \|v_i\|_{\infty, \mathcal{I}_i^D}^2 \right) \lesssim \delta_i^{-2} \left(\|v_i\|_{\infty, \Omega_i}^2 + \|v_i\|_{\infty, \mathcal{I}_i^D}^2 \right).$$

The Γ -norm terms are bounded similarly. For example

$$\frac{1}{2} \int_{\mathcal{I}_2^J} \int_{\mathcal{I}_1^J} (v_1(x) - v_1(y))^2 \gamma_{\delta_1}(x, y) dy dx \lesssim \delta_1^{-2} \left(|\mathcal{I}_2^J| \|v_1\|_{\infty, \mathcal{I}_2^J}^2 + |\mathcal{I}_1^J| \|v_1\|_{\infty, \mathcal{I}_1^J}^2 \right).$$

The remaining terms are handled analogously, leading to

$$\|v\|_{\Gamma}^2 \lesssim \max\{\delta_1^{-1}, \delta_2^{-1}\} \left(\|v\|_{\infty, \mathcal{I}_1^J}^2 + \|v\|_{\infty, \mathcal{I}_2^J}^2 \right).$$

Combining these estimates yields

$$\|v\|_{\delta}^2 \lesssim \max\{\delta_1^{-2}, \delta_2^{-2}\} \left(\|v\|_{\infty, \Omega_1 \cup \Omega_2}^2 + \|v\|_{\infty, \mathcal{I}_1^D \cup \mathcal{I}_2^D}^2 \right).$$

Taking square roots completes the proof.

Proof of Lemmas 3.2. For each subdomain Ω_i ($i = 1, 2$), the nonlocal Poincaré inequality [40, Theorem 3.34] implies

$$\|v_i\|_{L^2(\Omega_i)}^2 \leq C_{p,i} \|v_i\|_{\delta_i}^2, \quad \text{where } C_{p,i} = \frac{|\Omega_i|^2}{2\sigma_i}. \quad (29)$$

Since $v = 0$ on \mathcal{I}_i^D , it follows that $\|v\|_{\delta_i}^2 \leq \|v\|_{\delta}^2$. Summing over subdomains

$$\|v\|_{L^2(\Omega_1 \cup \Omega_2)}^2 = \|v_1\|_{L^2(\Omega_1)}^2 + \|v_2\|_{L^2(\Omega_2)}^2 \leq (C_{p,1} + C_{p,2}) \|v\|_{\delta}^2.$$

The lower bound follows by setting $C_1 = (C_{p,1} + C_{p,2})^{-1/2}$. For the upper bound

$$\|v\|_{\delta_i}^2 \leq 2 \int_{\Omega_i \cup \mathcal{I}_i^D} v_i^2(x) \left(\int_{\Omega_i \cup \mathcal{I}_i^D} \gamma_{\delta_i}(x, y) dy \right) dx \leq C_{l,i} \delta_i^{-2} \|v\|_{L^2(\Omega_i)}^2.$$

Similarly, for the Γ -norm

$$\|v\|_{\Gamma}^2 \leq C_{l,3} \max\{\delta_1^{-2}, \delta_2^{-2}\} (\|v\|_{L^2(\mathcal{I}_1^J)}^2 + \|v\|_{L^2(\mathcal{I}_2^J)}^2).$$

Combining these results gives

$$\|v\|_{\delta} \leq C_2 \max\{\delta_1^{-1}, \delta_2^{-1}\} \|v\|_{L^2(\Omega_1 \cup \Omega_2)},$$

which completes the proof.

Acknowledgments

H. Dong was partially supported by the National Natural Science Foundation of China (Grant No. 12001193), the Scientific Research Fund of Hunan Provincial Education Department (Grant No.24A0052), and the Hunan provincial national science foundation of China (No. 2024JJ6298). Z. Xie was supported by the National Natural Science Foundation of China (Grant No. 12171148, 52331002), the Major Program of Xiangjiang Laboratory (Grant No. 22XJ01013). J. Zhang was partially supported by National Natural Science Foundation of China (Grant No. 12571438) and the Fundamental Research Funds for the Central Universities (Grant No. 2042021kf0050).

References

- [1] S. A. Silling, Reformulation of elasticity theory for discontinuities and long-range forces, *J. Mech. Phys. Solids*, 48 (1) (2000) 175–209.
- [2] Y. D. Ha, F. Bobaru, Characteristics of dynamic brittle fracture captured with peridynamics, *Eng. Fract. Mech.*, 78 (6) (2011) 1156–1168.
- [3] S.-N. Roth, P. Léger, A. Soulaïmani, A combined XFEM-damage mechanics approach for concrete crack propagation, *Comput. Methods Appl. Mech. Engrg.*, 283 (2015) 923–955.
- [4] Y. Li, Y. Fu, A thermo-elasto-plastic model for a fiber-metal laminated beam with interfacial damage, *Appl. Math. Model.*, 39 (12) (2015) 3317–3330.
- [5] Q. Yang, B. Cox, Cohesive models for damage evolution in laminated composites, *Int. J. Fract.*, 133 (2005) 107–137.
- [6] Q. Du, Y. Tao, X. Tian, A peridynamic model of fracture mechanics with bond-breaking, *J. Elasticity*, 132 (2) (2018) 197–218.
- [7] J. Li, Q. Wang, Y. Zan, L. Ju, C. Jing, Y. Zhang, Research on wing crack propagation of closed crack under uniaxial compression based on peridynamics, *Eng. Anal. Bound. Elem.*, 158 (2024) 121–138.
- [8] C. Glusa, M. D’Elia, G. Capodaglio, M. Gunzburger, P. B. Bochev, An asymptotically compatible coupling formulation for nonlocal interface problems with jumps, *SIAM J. Sci. Comput.*, 45 (3) (2023) A1359–A1384.
- [9] S. A. Silling, R. B. Lehoucq, Peridynamic theory of solid mechanics, *Adv. Appl. Mech.*, 44 (2010) 73–168.
- [10] T. Mengesha, Q. Du, The bond-based peridynamic system with Dirichlet-type volume constraint, *Proc. Roy. Soc. Edinburgh Sect. A*, 144 (1) (2014) 161–186.

- [11] T. Mengesha, Q. Du, Characterization of function spaces of vector fields and an application in nonlinear peridynamics, *Nonlinear Anal.*, 140 (2016) 82–111.
- [12] A. Arroyo-Rabasa, Functional and variational aspects of nonlocal operators associated with linear PDEs, *Nonlinear Anal.* 251 (2025) Paper No. 113683, 26.
- [13] Q. Du, J. Zhang, C. Zheng, On uniform second order nonlocal approximations to linear two-point boundary value problems, *Commun. Math. Sci.*, 17 (6) (2019) 1737–1755.
- [14] J. Z. Yang, X. Yin, J. Zhang, On uniform second-order nonlocal approximations to diffusion and subdiffusion equations with nonlocal effect parameter, *Commun. Math. Sci.*, 20 (2) (2022) 359–375.
- [15] X. Tian, Q. Du, Asymptotically compatible schemes and applications to robust discretization of nonlocal models, *SIAM J. Numer. Anal.*, 52 (4) (2014) 1641–1665.
- [16] X. Tian, Q. Du, Analysis and comparison of different approximations to nonlocal diffusion and linear peridynamic equations, *SIAM J. Numer. Anal.*, 51 (6) (2013) 3458–3482.
- [17] Y. Tao, X. Tian, Q. Du, Nonlocal diffusion and peridynamic models with Neumann type constraints and their numerical approximations, *Appl. Math. Comput.*, 305 (2017) 282–298.
- [18] Q. Du, J. Yang, Asymptotically compatible Fourier spectral approximations of nonlocal Allen-Cahn equations, *SIAM J. Numer. Anal.*, 54 (3) (2016) 1899–1919.
- [19] Q. Du, J. Yang, Fast and accurate implementation of Fourier spectral approximations of nonlocal diffusion operators and its applications, *J. Comput. Phys.*, 332 (2017) 118–134.
- [20] Q. Du, L. Ju, J. Lu, A discontinuous Galerkin method for one-dimensional time-dependent nonlocal diffusion problems, *Math. Comp.*, 88 (315) (2019) 123–147.
- [21] Q. Du, L. Ju, J. Lu, X. Tian, Numerical analysis of a class of penalty discontinuous Galerkin methods for nonlocal diffusion problems, *ESAIM Math. Model. Numer. Anal.*, 58 (5) (2024) 2035–2059.
- [22] Q. Du, J. Yang, Z. Zhou, Analysis of a nonlocal-in-time parabolic equation, *Discrete Contin. Dyn. Syst. Ser. B*, 22 (2) (2017) 339–368.
- [23] Q. Du, X. Tian, Stability of nonlocal Dirichlet integrals and implications for peridynamic correspondence material modeling, *SIAM J. Appl. Math.*, 78 (3) (2018) 1536–1552.
- [24] Q. Du, H. Xie, X. Yin, J. Zhang, Error estimates of finite element methods for nonlocal problems using exact or approximated interaction neighborhoods (2024). [arXiv:2409.09270](https://arxiv.org/abs/2409.09270).
- [25] Q. Du, H. Xie, X. Yin, On the convergence to local limit of nonlocal models with approximated interaction neighborhoods, *SIAM J. Numer. Anal.*, 60 (4) (2022) 2046–2068.

- [26] C. S. Peskin, Numerical analysis of blood flow in the heart, *J. Comput. Phys.* 25 (3) (1977) 220–252.
- [27] C. S. Peskin, The immersed boundary method, *Acta Numer.*, 11 (2002) 479–517.
- [28] T.-P. Fries, T. Belytschko, The extended/generalized finite element method: an overview of the method and its applications, *Int. J. Numer. Meth. Eng.*, 84 (3) (2010) 253–304.
- [29] P. Hansbo, M. G. Larson, S. Zahedi, A cut finite element method for a stokes interface problem, *App. Numer. Math.*, 85 (2014) 90–114.
- [30] X. He, T. Lin, Y. Lin, Immersed finite element methods for elliptic interface problems with non-homogeneous jump conditions, *Int. J. Numer. Anal. Model*, 8 (2) (2011) 284–301.
- [31] T. Lin, Y. Lin, X. Zhang, Immersed finite element method of lines for moving interface problems with nonhomogeneous flux jump, *Contemp. Math.*, 586 (2013) 257–265.
- [32] T. Lin, Y. Lin, X. Zhang, Partially penalized immersed finite element methods for elliptic interface problems, *SIAM J. Numer. Anal.*, 53 (2) (2015) 1121–1144.
- [33] W. Ying, C. S. Henriquez, A kernel-free boundary integral method for elliptic boundary value problems, *J. Comput. Phys.*, 227 (2) (2007) 1046–1074.
- [34] W. Ying, W.-C. Wang, A kernel-free boundary integral method for implicitly defined surfaces, *J. Comput. Phys.*, 252 (2013) 606–624.
- [35] B. Alali, M. Gunzburger, Peridynamics and material interfaces, *J. Elasticity*, 120 (2) (2015) 225–248.
- [36] P. Seleson, M. Gunzburger, M. L. Parks, Interface problems in nonlocal diffusion and sharp transitions between local and nonlocal domains, *Comput. Meth. Appl. Mech. Engrg.*, 266 (2013) 185–204.
- [37] G. Capodaglio, M. D’Elia, P. Bochev, M. Gunzburger, An energy-based coupling approach to non-local interface problems, *Comput. & Fluids*, 207 (2020) 104593, 12.
- [38] Y. Yu, H. You, N. Trask, An asymptotically compatible treatment of traction loading in linearly elastic peridynamic fracture, *Comput. Meth. Appl. Mech. Engrg.*, 377 (2021) Paper No. 113691, 36.
- [39] Y. Fan, H. You, X. Tian, X. Yang, X. Li, N. Prakash, Y. Yu, A meshfree peridynamic model for brittle fracture in randomly heterogeneous materials, *Comput. Meth. Appl. Mech. Engrg.*, 399 (2022) Paper No. 115340, 36.
- [40] Q. Du, *Nonlocal modeling, analysis, and computation*, SIAM, Philadelphia, PA, 2019.